Electron-impact ionization of atomic hydrogen: Comparison of asymmetric $(e,2e)$ measurements with theories

B. Lohmann, I. E. McCarthy, A. T. Stelbovics, and E. Weigold
Institute for Atomic Studies, School of Physical Sciences, The Flinders University of South Australia, Adelaide, South Australia 5042, Australia
(Received 14 December 1983)

Differential cross sections have been measured for the electron-impact ionization of atomic hydrogen, using the $(e,2e)$ technique with coplanar asymmetric kinematics. The experiments were performed at an incident energy of 250 eV with the slow outgoing electron being detected at energies of 5, 10, and 14 eV, for scattering angles of the fast outgoing electron of 3°, 5°, and 8°. The data are compared with differential cross sections calculated with use of the factorized distorted-wave impulse approximation, the plane-wave impulse approximation, and three recent Born-approximation calculations, consisting of first-order Born, second-order Born, and eikonal Born series treatments. In the distorted-wave impulse approximation calculations we investigate the effect of using different descriptions for the fast outgoing electron. Comparison of the data and the calculated cross sections indicates reasonable agreement with the distorted-wave impulse calculations, and good agreement with the second-order and eikonal Born series calculations.

INTRODUCTION

In the $(e,2e)$ reaction the kinematics of an electron-impact ionizing event is fully determined. The energy (E_0) and direction of the incident electron are known, and the energies E_A and E_B and directions of motion (θ_A,ϕ_A) and (θ_B,ϕ_B) relative to the incident direction of the two electrons emerging from the ionizing collision are determined. The momenta of the incident and two outgoing electrons, $\vec{k}_0$, $\vec{k}_A$, and $\vec{k}_B$, are therefore known. The technique has been used in detailed investigations of both the bound state structures of atoms and molecules,[1-3] and the reaction mechanism of the ionization process in atomic targets.[4-8]

The experiments may be divided into two broad kinematic regimes. The first is symmetric kinematics in which the outgoing electrons are detected with equal energies $E_A=E_B$ and at equal polar angles $\theta_A=\theta_B$, and the second, asymmetric kinematics in which $E_A \gg E_B$ and $\theta_A \ll \theta_B$. At high incident energies the experiments in the symmetric regime, in particular those employing noncoplanar symmetric kinematics, yield bound-state information in the form of momentum probability distributions and separation energy spectra,[1-3] while those experiments with asymmetric kinematics may be used to probe the ionization reaction mechanism in some detail.

Measurements of the $(e,2e)$ differential cross section in the asymmetric kinematic regime provide a fundamental testing ground for various theoretical approaches to the ionization problem. With a target of atomic hydrogen the ionization problem is greatly simplified, since the bound-state wave functions are known exactly, as are the two-body potentials within the three-body system. We have a pure three-body problem with known forces, namely, the three-body Coulomb problem. The detailed understanding of electron-impact ionization of atomic hydrogen is therefore of great fundamental interest. It provides the simplest testing ground for any theory of ionization, and is the ideal testing ground for the solution of the quantum-mechanical three-body system. It should therefore prove to be of great heuristic value. In treating the problem of electron-impact ionization of atomic hydrogen the major theoretical thrust must be concerned with developing a better description of the incident channel, of the three-body final state, and of the collision process.

Weigold *et al.*[4] measured the $(e,2e)$ differential cross sections in atomic hydrogen at impact energies of 100, 113.6, 250, and 413.6 eV for a variety of emitted electron energies and angles, using both symmetric and asymmetric kinematics. Their results were compared with the factorized distorted-wave impulse approximation (DWIA), the plane-wave impulse approximation (PWIA), and the plane-wave Born approximation with exchange (PWBE). In the DWIA calculations they explored the form of the final three-body state by treating the two outgoing electrons in several different ways.

In this paper we present recent results which extend their measurements to more asymmetric conditions in order to provide more stringent tests for theory. These experiments were performed at an incident energy of $E_0=250$ eV. The slow outgoing electron was detected with energies $E_B=5$, 10, and 14 eV. The angular correlations were obtained at three different values of the scattering angle of the fast electron, $\theta_A=3°$, 5°, or 8°.

Using similarly extreme asymmetric conditions Ehrhardt *et al.*[5-7] have produced extensive measurements of the $(e,2e)$ differential cross section for helium. They found that the angular correlations obtained in these experiments exhibit two peaks, now commonly called the binary encounter and the recoil peak. The binary encounter peak is predominantly the result of a close electron-electron collision and is in the approximate direction of the momentum transfer, $\vec{K}=\vec{k}_0-\vec{k}_A$, where $\vec{k}_A$ is the momentum of the fast scattered electron. That is, the

slow ejected electron is scattered along the momentum transfer direction, hence the term "binary." The recoil peak is essentially the result of interactions with the ion. In the recoil peak, the electron emerges approximately antiparallel to the momentum transfer direction, hence the terminology "recoil."

The measurements of Ehrhardt *et al.* have been compared with a number of theoretical calculations, including first- and second-order Born calculations, distorted-wave Born calculations, and Green's-function calculations.[9–12]

We have carried out a number of factorized distorted-wave impulse approximation calculations and a plane-wave impulse approximation calculation, and compare them with the present measurements. In the DWIA calculations we investigate the effect of using three different descriptions of the fast outgoing electron wave. The data are also compared with the recent three Born-approximation calculations of Byron, Joachain, and Piraux,[13] namely, the first-order Born approximation, the second-order Born approximation, and the eikonal Born series.

THEORETICAL BACKGROUND

The scattering amplitude for the three-body problem of ionization of atomic hydrogen is defined by

$$M=\langle\Phi^{(-)}\,|\,T\,|\,\Phi^{(+)}\rangle\ , \tag{1}$$

where T is the three-body T matrix for the electron-hydrogen system. The wave functions $\Phi^{(\pm)}$ are the asymptotic wave functions for the system, where the superscripts $(\pm)$ indicate incoming and outgoing boundary conditions, respectively. The two-body potentials in the system are v_1, v_2, and v_3, where v_1 is the potential between the incident electron and the ion, v_2 is the potential between the bound electron and the ion, and v_3 is the interelectron potential (we indicate the incoming electron by the subscript 1 and the bound electron by the subscript 2).

Using the Lippmann-Schwinger equation, the three-body T matrix may be written, in terms of these potentials and the Green's function G, for the system as

$$T=V+VGV \tag{2}$$

$$=(v_1+v_3)+(v_1+v_3)G(v_1+v_3)\ , \tag{3}$$

where we have partitioned the Hamiltonian such that

$$V=v_1+v_3\ . \tag{4}$$

Introducing the Green's function G_0 for the interaction of the target electron with the proton, we may iterate this equation to produce

$$T=(v_1+v_3)+(v_1+v_3)G_0(v_1+v_3)+(v_1+v_3)G_0(v_1+v_3)G_0(v_1+v_3)+\cdots \tag{5}$$

which is simply the Born series expansion for the three-body T matrix. Taking as an approximation to the T matrix the first term of the above expansion yields the first-order Born ($B1$) approximation.

The scattering amplitude in this approximation may be written

$$M_{B1}=\langle\vec{k}_A\chi^{(-)}(\vec{k}_B)\,|\,v_1+v_3\,|\,\psi_i\vec{k}_0\rangle\ , \tag{6}$$

where ψ_i is the bound state of the target, in this case the ground state of atomic hydrogen. $\chi^{(-)}(\vec{k}_B)$ is a distorted wave which in practice may be approximated by a plane wave or a Coulomb wave.

Including both first- and second-order terms of the Born expansion in the approximation to the T matrix yields the second Born approximation ($B2$)

$$M_{B2}=\langle\vec{k}_A\chi^{(-)}(\vec{k}_B)\,|\times[(v_1+v_3)+(v_1+v_3)G_0(v_1+v_3)]\,|\,\psi_i\vec{k}_0\rangle\ . \tag{7}$$

The eikonal-Born-series calculation attempts the logical extension to third order in the Born expansion by approximating the third-order Born term in the scattering amplitude by the third-order term of an eikonal multiple scattering (Glauber) expansion.[14]

In the impulse approximation the three-body T matrix is approximated by the first order term of the Faddeev-Watson multiple scattering expansion for the T matrix. That is,

$$T=t_1+t_3 \tag{8}$$

In the distorted-wave impulse approximation calculations presented here, the T matrix is taken to be independent of the ion coordinates (binary encounter approximation). Thus

$$T=t_3\ . \tag{9}$$

The scattering amplitude in the full DWIA is then

$$M_{\mathrm{DWIA}}=\langle\chi^{(-)}(\vec{k}_A)\chi^{(-)}(\vec{k}_B)\,|\,t_3\,|\,\psi_i\chi^{(+)}(\vec{k}_0)\rangle\ . \tag{10}$$

The above form of the scattering amplitude involves a nine-dimensional integral. Numerical implementation of Eq. (10) involves using the factorization approximation[2] which yields

$$M=\langle\vec{k}'\,|\,t_m\,|\,\vec{k}\rangle\langle\chi^{(-)}(\vec{k}_A)\chi^{(-)}(\vec{k}_B)\,|\,\psi_i(\vec{q})\chi^{(+)}(\vec{k}_0)\rangle\ , \tag{11}$$

where $\vec{q}$ is the ion (proton) recoil momentum $\vec{k}_0-\vec{k}_A-\vec{k}_B$, t_m is the two-body electron-electron Coulomb t matrix with exchange for spin state m, and

$$\vec{k}'=\tfrac{1}{2}(\vec{k}_A-\vec{k}_B)\ , \tag{12}$$

$$\vec{k}=\tfrac{1}{2}(\vec{k}_0+\vec{q})\ . \tag{13}$$

Once we have determined the appropriate form of the scattering amplitude, the $(e,2e)$ cross section is simply

$$\frac{d^5\sigma}{d\Omega_A d\Omega_B dE_A}=(2\pi)^4\frac{k_A k_B}{k_0}\sum_m|M|^2\ , \tag{14}$$

where $\sum_m$ stands for the sum over final and average over initial spin states.

In the DWIA calculations reported here the distorted

waves representing the incident and slow outgoing electrons, $\chi^{(+)}(\vec{k}_0)$ and $\chi^{(-)}(\vec{k}_B)$, have been calculated as follows. The incident electron is in each case represented as a distorted wave calculated in the static interaction potential, including exchange, for the ground state of atomic hydrogen.[15] The slow electron is in each case represented by a Coulomb wave with effective charge $Z=-1$. As the fast scattered electron is far more energetic than the slow ejected electron ($E_A \gg E_B$), it is reasonable to assume that the fast electron will be long gone from the vicinity of the target before the slow electron has moved an appreciable distance from the ion. Thus we expect the potential seen by the slow electron to be essentially a bare Coulomb potential. Hence the choice of a Coulomb wave to represent the slow electron.

The distorted wave used to represent the fast outgoing electron $\chi^{(-)}(\vec{k}_A)$ was calculated in three different ways. The DWIA calculations involving the three forms for the distorted wave are labeled DWIA-I, DWIA-II, and DWIA-III. In the DWIA-I, the fast outgoing electron is represented in the same way as the incident electron, that is, a distorted wave calculated in the static interaction potential for the ground state of atomic hydrogen. The justification for using this approximation is that, due to the large disparity in energy of the two outgoing electrons, the fast electron will be well away from the target system before the slow electron can move an appreciable fraction of a Bohr radius. Hence the fast outgoing electron will basically "see" a hydrogen atom in its ground-state configuration until it is far enough from the target that the potential it feels is negligible. In the DWIA-II the fast electron is represented as a plane wave $\vec{k}_A$, and in the DWIA-III the fast electron is represented as a Coulomb wave. Thus the DWIA-II and DWIA-III represent two extreme cases; in one the proton potential is fully screened by the slow electron and the fast electron experiences no potential at all, and in the other it is assumed that the slow electron does not screen the proton potential at all, so that the fast electron sees simply a bare proton. One might expect the DWIA-I to be the better approximation at very low slow-electron energies, with the DWIA-III becoming more pertinent as the slow-electron energy increases.

The approximation to the three-body T matrix in the DWIA does not include the ion coordinates. In order to describe the recoil peak in the $(e,2e)$ cross section for the asymmetric experiments, the effect of the ion must enter through the distorted waves (since the recoil peak is the result of interactions with the ion). Thus we would expect that the PWIA, in which the incoming and outgoing distorted waves in Eq. (11) are replaced by plane waves, would be incapable of predicting recoil peak. The results of a PWIA calculation are also presented for comparison.

EXPERIMENTAL DETAILS

The asymmetric $(e,2e)$ experiments were performed in the coplanar spectrometer, which has been described in detail elsewhere,[4] so only a brief description will be given here. The apparatus is shown schematically in Fig. 1.

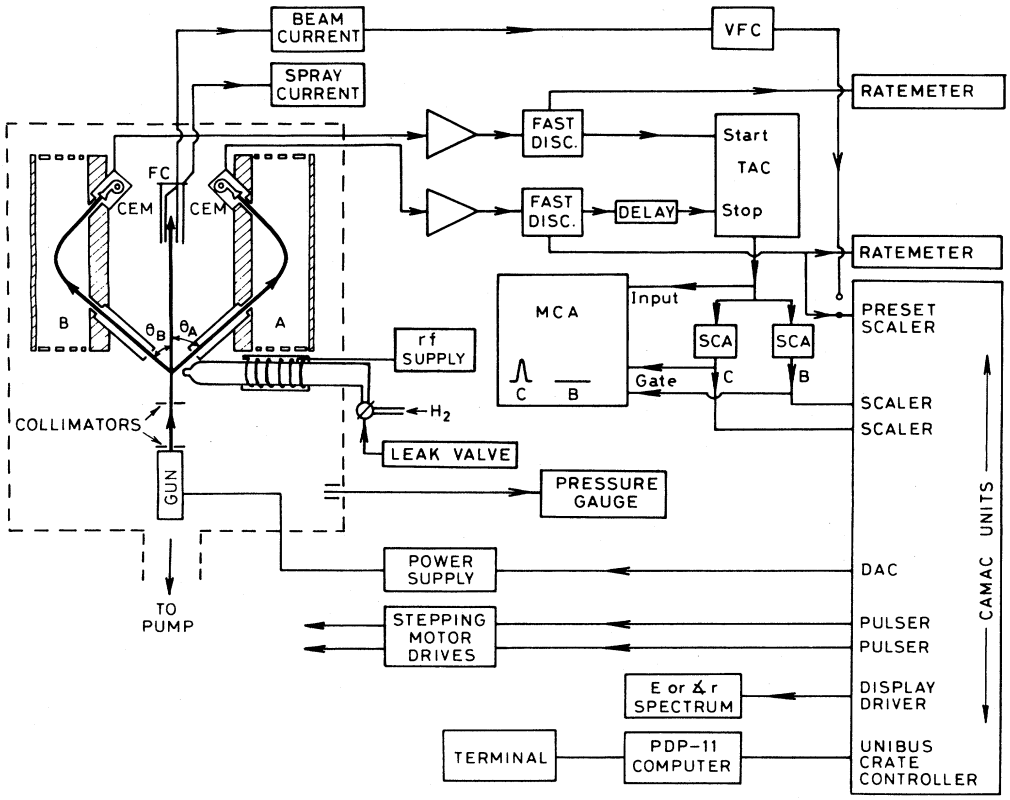

FIG. 1. Schematic diagram of the $(e,2e)$ spectrometer and associated fast timing and data-processing electronics.

Two cylindrical mirror analyzers are used to determine the energies of the two emitted electrons. The analyzers are mounted on two concentric turntables, which may be rotated independently by computer-controlled stepping motors. The entire experiment is computer controlled, including setting of energies and angles and data accumulation. Conventional fast timing electronics are used.[2,4] The electron gun used to produce the incident beam of electron is of conventional design and employs a thoriated tungsten wire filament. At an incident energy of 250 eV it produces approximately 3 μA of current focused into a 1.5-mm-diam collimated beam.

The atomic hydrogen used as the target in these experiments was produced in an rf discharge source. The source design was based upon designs used by Toennies *et al.*[16] and Slevin and Stirling.[17] The discharge tube and the surrounding coolant jacket were constructed from Pyrex. The rf coil which surrounds the tube and jacket is incorporated in the form of a coaxial resonator. The resonator consists of an inner coil surrounded by a coaxial copper cylinder. One end of the coil is free, the other end is connected to the grounded outer copper cylinder. The rf power is tapped into the coil at a position which results in the least reflected power. This position was determined by trial and error. We found we could not achieve a good impedance match with water in the coolant jacket, so alternative liquids were considered, with kerosene being the final choice because of its low dielectric constant. The rf supply used to power the discharge was a 100-W, variable-frequency (10—45 MHz) supply. We operated the discharge at approximately 41 MHz and a power input of 25 W. The dissociation fraction of atomic hydrogen in the discharge was typically (70—80)%, and the coincidence separation energy spectrum show a peak at 13.6 eV from H and a much smaller peak at 15.9 eV due to H_2. No background (other than the usual accidental coincidence events) were found to contribute to the atomic hydrogen events (see Ref. 4 for details).

The Auger lines in argon were used to calibrate the cylindrical mirror analyzers to ensure an accurate measurement of the energies of the emitted electrons. With an incident energy of 1 keV, the Auger lines were observed by measuring the count rate in each analyzer at a fixed scattering angle as a function of the voltage on the back plate of the analyzer, the analyzer pass energy being kept constant. The peaks and energy scale in the Auger spectrum were identified using the data of Mehlhorn and Stahlherm.[18] The analyzers were calibrated at the energy of the $L_3M_{23}M_{23}\,{}^1D_2$ Auger line in argon, namely, 203.26 eV. The relationship between "back-plate" voltage and the energy of the electrons transmitted by the analyzer was measured by elastic scattering from hydrogen and found to be extremely linear over the energy range from 30 to 300 eV, the lower energy being the limit of operation of the electron gun used in the present experiments. To calibrate the "slow-electron" analyzer at 5, 10, and 14 eV we simply extrapolated to the appropriate back-plate voltages.

The angular correlations were obtained by fixing the position of the fast-electron analyzer (θ_A) and varying the polar angle θ_B of the other analyzer, the coincidence count rate being measured as a function of θ_B. Each experimental run consisted of many scans over the whole range of angles θ_B, the time at each point being determined by a fixed preset count in the stationary fast-electron channel. When measuring the binary peak of the angular distribution, the two coplanar analyzers were in the $\phi_A=0,\phi_B=\pi$ position, that is, on opposite sides of the incident beam direction. When measuring the recoil peak, both analyzers were on the same half of the scattering plane, i.e., $\phi_A-\phi_B=0$. The analyzer used to detect the fast electron is moved from $-\theta_A$ to $+\theta_A$ when changing from binary to recoil peak measurements. This means that we use the same analyzer to measure the slow-electron energy in both the binary and recoil situations, thus removing any need for a transmission correction before normalizing the experimental data in the two angular regions studied. This normalization was carried out by measuring the coincidence count rates at a fixed angle θ_B, changing the setting of the fast-electron analyzer from $\theta_A,\phi_A=0$ to $\theta_A,\phi_A=\pi$ (i.e., $\theta_A\rightarrow-\theta_A$), the slow-electron detector providing the present signal.

Although the experiments are not absolute, we measured the relative normalizations between the data for the different energies E_A and E_B and the different values of the scattering angles θ_A ($E_B=5$, 10, and 14 eV; $\theta_A=3°,5°,8°$). The energy normalizations were obtained by measuring the coincidence count rate for fixed θ_A and $\theta_B=70°$ (on the binary peak), while varying the energies of the slow and fast outgoing electrons, keeping their sum constant. The normalization as a function of angle for fixed electron energies was obtained by measuring the count rate at $\theta_B=70°$ on the binary peak as a function of the scattering angles of the fast electron. A further normalization run was carried out in which both θ_A and E_A (and E_B) were varied. The information obtained from these independent measurements provided a cross check on the accuracy (better than 10%) of the relative normalizations.

The pass energy of the analyzer used to detect the slow outgoing electron was kept constant for all three selected energies, being fixed at 28 eV. The voltages on the decelerating lens were adjusted to give the optimum count rates at each energy, and were subsequently not varied. In these circumstances the transmission efficiency of the analyzer should be essentially independent of the slow-electron energies, $E_B=5$, 10, and 14 eV. In order to check that this was indeed the case, we measured the double differential cross sections in helium at an incident energy of 250 eV and a scattering angle of 70°, and determined the relative cross section at the different energies. Our results were compared with recent measurements (interpolated to 250 eV) by Sharp[19] and Opal, Beaty, and Peterson,[20] and with recommended distributions produced by Kim.[21] The measurements confirmed that the analyzer efficiency was independent of energy over the range 5—14 eV.

A correction to the angular distribution obtained by analyzer B (which detects the slow electron) may be necessary in the situation where the analyzer does not see the full collision volume at all angles. The fixed (fast-electron) analyzer A is positioned at a much smaller polar

angle relative to the incident beam than is the analyzer B. Analyzer A thus views a longer length of the electron beam than does analyzer B. If analyzer A views the whole of the collision length, analyzer B must also view the whole of the collision length at all angles θ_B if there is to be no correction. In a coincidence experiment, the collision volume which needs to be covered by analyzer B may be reduced by restricting the aperture of the fixed detector. However, in our experiments the aperture at the entrance to analyzer A was large enough to permit this analyzer to view the entire collision length. Our choice of apertures and geometry was such that we expected analyzer B to view the whole of the collision volume at all angles. We checked this by measuring the double differential cross section in helium at an incident energy of 200 eV for outgoing electron energies (E_B) of 10 eV. The incident energy, and hence electron beam profile, was selected to be close to that used in the present experiments on hydrogen, the outgoing electron energy (10 eV) being the central energy of the slow electron (E_B) in the present measurements. The angular distribution of the 10-eV electrons was compared with those obtained by Shyn and Sharp,[19] Opal *et al.*[20] and Kim.[21] The results confirmed that no angular correction was necessary over the angular range of interest ($50° \leq \theta_B \leq 120°$).

RESULTS AND DISCUSSION

Weigold *et al.*[4] compared their measurements of $(e,2e)$ differential cross sections in atomic hydrogen with both distorted-wave and plane-wave theories. The most asymmetric conditions employed in these measurements were $E_0=100$ eV, $E_B=25$ eV, $\theta_A=20°$ and $E_0=250$ eV, $E_B=50$ eV, $\theta_A=15°$. All the plane-wave theories gave very poor fits to their data. Four different factorized distorted-wave impulse approximations were considered. Their calculation DWIA-1 treated both outgoing electrons as Coulomb waves of full effective charge, $Z=-1$. In their DWIA-2 calculation the effective charges were dependent on angle of emission and determined by asymptotic constraints. Their calculation denoted by DWIA-3 used a constant average effective charge for each electron. Finally, their DWIA-4 calculation used a Coulomb wave for the slow emitted electron ($Z=-1$) and for the fast electron a distorted wave calculated in an energy-dependent ground-state optical model potential,[15] incorporating the static interaction potential and a term describing polarization and absorption. The incident electron in each of the above DWIA calculations was represented by a distorted wave calculated in this full optical model potential.

Weigold *et al.* found that the DWIA-2, in which effective charges determined by asymptotic conditions were used, gave a poorer description of the data than the DWIA-1 calculation in which effective charges $Z_A=Z_B=-1$ were used, indicating that the cross section is most sensitive to the form of the wave functions in the interaction region, and not to asymptotic conditions. For some values of the momentum transfer the DWIA-3 with average effective charges somewhat smaller than unity gave better results than the DWIA-1. The DWIA-4 gave reasonable agreement with the data and, as might be expected, was particularly good in those experiments with the most asymmetric conditions.

In the present experiments we have measured $(e,2e)$ differential cross sections for atomic hydrogen at an incident energy of 250 eV, with slow-electron energies of $E_B=5$, 10, and 14 eV and scattering angles for the fast electron of $\theta_A=3°$, 5°, and 8°. The data are presented in Table I. Although the measurements are not absolute but are normalized relative to each other, they have been put on an absolute scale in Table I by normalizing the binary peak at $\theta_B=70°$ of the $E_B=10$ eV, $\theta_A=5°$ data to the recent second-Born-approximation calculations of Byron, Joachain, and Piraux.[13] A line of best fit through the data was used to determine the $\theta_B=70°$ cross section. The data are plotted in Figs. 2 and 3 in the form of polar plots. In Fig. 2 the present measurements have been normalized to the second-Born-approximation calculations as outlined above, while in Fig. 3 the measurements have been normalized to the DWIA calculations by taking a line of best fit through the $E_B=10$ eV, $\theta_A=5°$ data and setting the cross section at the $\theta_B=70°$ point equal to 1.0 a.u. This gives a reasonable overall fit of the measurements to the various DWIA calculations at the different energies and angles.

In Fig. 2 the measured $(e,2e)$ cross sections are compared with recent second-Born-approximation, first-Born-approximation, and eikonal-Born-series (EBS) calculations of Byron *et al.*[13] In the second-Born-approximation calculation the second-order Born term in the scattering amplitude was calculated in an approximate way by replacing the target excitation energies by an average excitation energy, the sum over intermediate states then being carried out with the use of closure. This could be expected to be a reasonable approximation since the ejected electron has low energy. In the full EBS calculation the second-Born-approximation term was computed with more accuracy by including exactly the contributions of the $1s$, $2s$, and $2p$ target states, the remaining states being included as before by using an average excitation energy. In addition, the third-order Glauber term was included in the scattering amplitude.

The second-Born-approximation results give a very good fit to the binary peaks of the data, but underestimate the magnitude of the recoil peaks, an effect which is most pronounced in the $E_B=10$ eV, $\theta_A=5°$ case [Fig. 2(d)]. The relative magnitudes of the binary peaks are predicted quite well. The second-Born-approximation treatment works best in the $\theta_A=3°$, $E_b=5$ eV case, where it gives essentially the correct magnitudes and shapes of both the recoil and binary peaks. This corresponds to the case of smallest momentum transfer, $K=0.27$ a.u., where the Born approximation is expected to be most accurate. The EBS results also give reasonable fits to the data, being very similar to those of the second-Born-approximation treatment. The EBS results actually give a slightly better description of the data, the recoil to binary peak height ratios being larger than those given by the second-Born-approximation calculation, but not as large as those observed experimentally. The EBS calculation is also best in

TABLE I. The 250-eV ($e,2e$) cross sections for hydrogen normalized to the second-order Born calculations (Ref. 13) at $E_B=10$ eV, $\theta_A=5°$, $\theta_B=70°$, $\phi_A-\phi_B=\pi$ as discussed in the text. Numbers in parentheses indicate the one-standard-deviation errors in the last significant figures.

				$\phi_A-\phi_B=\pi$			
θ_B	$E_B=5$ eV $\theta_A=3°$	$E_B=5$ eV $\theta_A=5°$	$E_B=5$ eV $\theta_A=8°$	$E_B=10$ eV $\theta_A=5°$	$E_B=10$ eV $\theta_A=8°$	$E_B=14$ eV $\theta_A=5°$	$E_B=14$ eV $\theta_A=8°$
40	7.61(1.34)	4.98(67)	1.76(54)	1.45(48)		1.90 (33)	
45	8.95(1.34)	3.68(67)	1.67(54)	2.44(49)		1.92(33)	
50	10.63(1.38)	4.98(67)	1.30(54)	2.44(31)	1.00(25)		
52.5						1.98(25)	
55	9.29(1.51)	5.31(67)	2.55(59)	2.33(30)	1.34(22)		
60	11.09(1.55)	7.03(67)	2.68(54)	2.52(30)	1.82(22)	2.12(34)	1.28(18)
65	9.29(1.38)	7.20(67)	3.77(54)	3.18(30)	2.15(22)	2.26(34)	1.38(18)
70	10.59(1.38)	6.07(63)	2.92(50)	2.70(30)	2.09(22)	1.78(33)	1.87(18)
75	9.25(1.34)	6.95(63)	3.77(46)	3.39(31)	2.37(23)	2.20(33)	1.68(17)
80	6.86(1.21)	5.44(59)	3.51(46)	2.87(20)	2.27(23)	1.78(32)	1.73(17)
85	9.71(1.26)	6.07(59)	4.10(42)	2.65(20)	2.39(23)	1.41(30)	2.13(19)
90	5.69(1.17)	5.56(54)	3.39(42)	2.38(20)	2.13(23)	1.09(29)	1.69(20)
95	7.57(1.21)	3.85(54)	2.80(42)	1.65(19)	2.06(23)	1.18(29)	1.84(20)
100	3.22(1.13)	5.27(59)	1.92(42)	1.64(19)	2.00(23)	0.86(28)	1.50(21)
105	3.89(1.13)	3.93(63)	2.22(42)	1.65(28)	1.56(23)	0.45(26)	1.11(22)
110		3.68(67)	2.01(50)	0.99(28)	1.49(23)	0.66(28)	0.76(23)
112.5	2.76(1.09)						
115		2.76(88)	1.46(71)	1.00(31)	1.11(23)		1.11(23)
117.5						0.61(21)	
				$\phi_A-\phi_B=0$			
50		0.33(50)		0.43(15)		0.27(25)	0.079(63)
52.5	0.59(71)						
55			0.07(23)	0.45(15)	0.34(11)	0.33(26)	0.126(59)
57.5		0.79(46)					
60	0.38(84)			0.39(14)	0.08(11)	0.82(26)	0.075(59)
65	2.05(92)		0.09(23)	0.25(14)	0.20(11)	0.38(21)	0.100(59)
67.5		1.09(46)					
70	0.92(92)		0.07(23)	0.22(15)	0.03(10)		0.050(59)
72.5						0.10(26)	
75	1.67(88)	0.84(46)	0.09(23)	0.38(15)	0.22(10)		0.126(59)
80	2.89(88)	1.26(50)	0.25(23)	0.53(15)	0.14(10)	0.75(25)	
82.5							0.013(54)
85	1.51(84)	0.75(50)	0.37(23)	0.60(15)	0.01(10)	0.68(26)	
90		2.22(50)	0.49(23)	0.71(15)	0.22(10)	1.10(26)	0.017(50)
92.5	3.47(79)						
95		1.92(50)	0.17(23)	0.83(15)	0.17(10)	0.84(26)	0.062(50)
100	2.80(84)	1.46(50)	0.17(23)	0.89(15)	0.19(11)		0.038(54)
102.5						0.74(21)	
105	5.10(88)	2.93(54)	0.68(23)	1.09(15)	0.13(11)		0.075(50)
110	3.57(88)	2.30(59)	0.62(25)	0.94(15)	0.01(11)	0.86(24)	0.151(50)
115	4.98(02)	3.22(67)	0.64(26)	1.32(16)	0.25(11)		0.134(54)
117.5						0.97(21)	
120	5.27(100)	2.51(71)	0.86(29)		0.11(11)		

the case with lowest momentum transfer, namely, $E_B=5$ eV and $\theta_A=3°$. The first-Born-approximation results consistently give much smaller recoil peaks than the other two calculations, and also predict axial symmetry about the direction of the momentum transfer $\vec{K}$, an effect which is not observed experimentally.

In contrast to the Born approximations, which are expected to be most accurate for the low momentum transfer situations, the impulse approximations are expected to be most valid for the large momentum transfer situations, i.e., close electron-electron collisions. Indeed, the impulse approximation was designed to describe symmetric collisions, which with an incident energy of 250 eV and $E_A=E_B$ and $\theta_A=\theta_B\sim45°$ involves collisions with $K\sim3$ a.u., i.e., momentum transfers an order of magnitude greater than those involved in the present measurements.

In Fig. 3 the three distorted-wave impulse approxima-

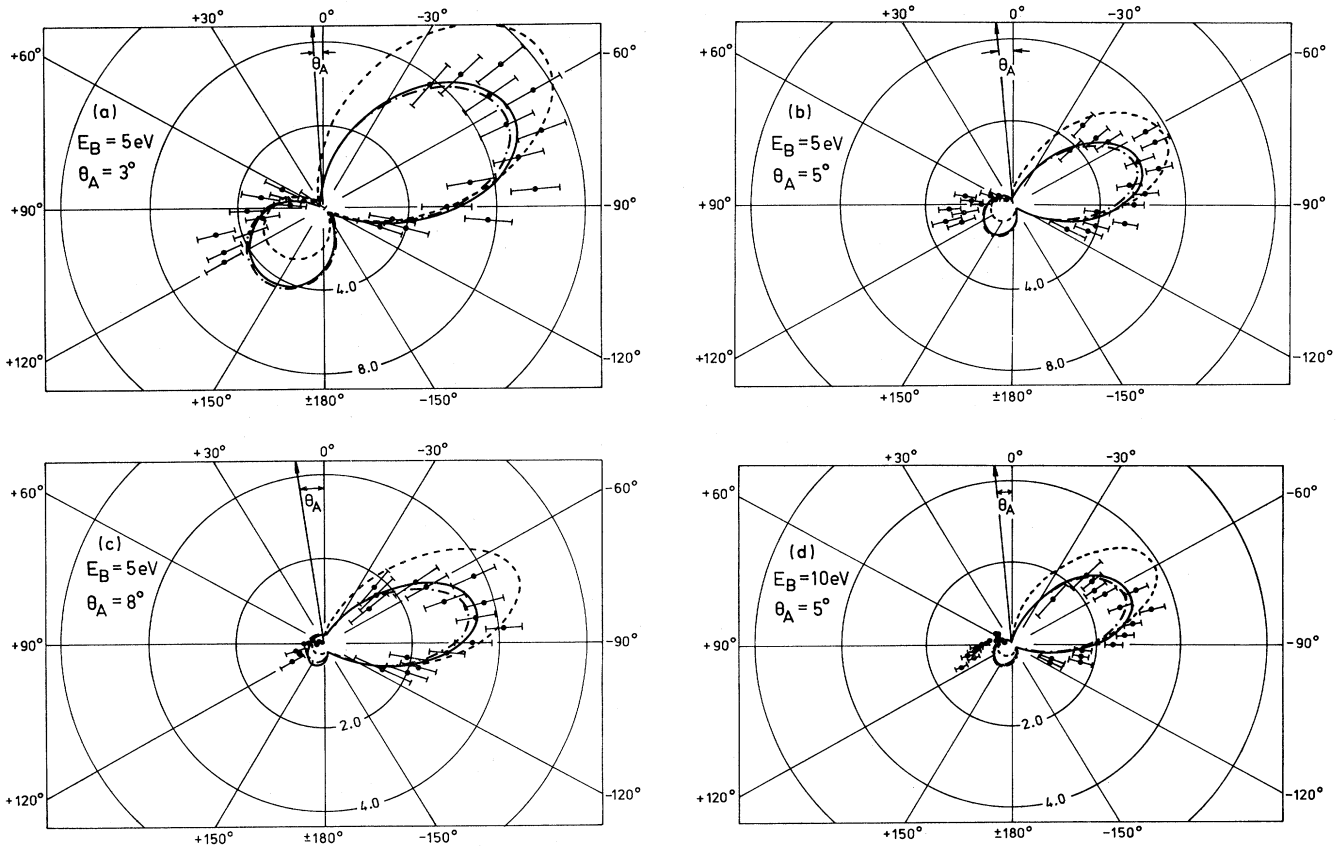

FIG. 2. Polar diagrams of the differential coplanar asymmetric ($e,2e$) cross sections measured for atomic hydrogen at $E_0=250$ eV with $E_B=5$ eV and $\theta_A=3°$, 5°, and 8° [(a)—(c), respectively] and $E_B=10$ eV and $\theta_A=5°$ (d). Data has been normalized to the second-order Born calculation at $E_B=10$ eV, $\theta_A=5°$ (see text for details). Calculated cross sections are — — —, first-order Born approximation; ——, second-order Born approximation; —·—·—·, eikonal Born series (Ref. 13). Cross sections are in atomic units.

tion calculations are presented, the data being normalized as discussed above. For the $E_B=10$ eV, $\theta_A=5°$ case [Fig. 3(d)] the DWIA-I calculation, in which the fast outgoing electron is represented by a distorted wave calculated in the static potential of the target, gives a good description of both the binary and recoil peaks. At $E_B=5$ eV, the DWIA-I gives a good description of the shape and direction of the binary peak at all angles, but at $\theta_A=3°$ it underestimates the magnitude of the binary peak, while at $\theta_A=8°$ it overestimates it. The recoil peak is quite well described in the $\theta_A=5°$ and 8° cases, but at $\theta_A=3°$ (the smallest momentum transfer case) the theory overestimates the magnitude of the recoil peak significantly. At $E_B=14$ eV, $\theta_A=5°$ the DWIA-I also gives a good description of the binary peak in shape and direction, but gives a smaller magnitude than is observed experimentally. The recoil peak predicted by the DWIA-I is also somewhat smaller than the observed recoil peak. For both $E_B=10$ and 14 eV and the scattering angle of 8°, the calculation gives the binary peak farther forward than observed. However, the DWIA-I calculation predicts the magnitude of the binary peak rather well at $E_B=14$ eV but overestimates it at $E_B=10$ eV. In both cases the recoil peak is described very well. The DWIA-I treatment obviously does best for situations involving the largest momentum transfer. Some of the DWIA-I calculations show a significant bulge in the recoil peak at $\theta_B=30°$—60°. This bulge is not obvious in the experimental data.

The results of the DWIA-II calculation, in which the fast electron is treated as a plane wave, are rather similar to the DWIA-I results, except that the magnitude of the binary peak is larger than that given by the DWIA-I calculation, and the binary peaks are moved to smaller values of θ_B. In addition, the bulge observed in the recoil peak DWIA-I cross sections are not present in the DWIA-II results. In the DWIA-III calculation the fast outgoing electron is treated as a Coulomb wave, which is an unrealistic approximation in the asymptotic regions since the slow electron will effectively screen the fast electron from the full effect of the proton potential. We would expect the fast electron to experience in reality a potential which is intermediate between that due to a neutral atom and that due to a bare iron. The DWIA-III calculation gives smaller binary peak cross sections than the other two DWIA calculations, and the peak is moved to more backward angles. The recoil peaks in this calculation show a pronounced double-lobe structure, with one lobe being in the "normal" recoil peak position, and the other peaking at $\theta_B\sim 40°$—50°. This second lobe appears to be an enlarged version of the bulge in the recoil peak seen in the DWIA-I results. Its presence in the DWIA-III and

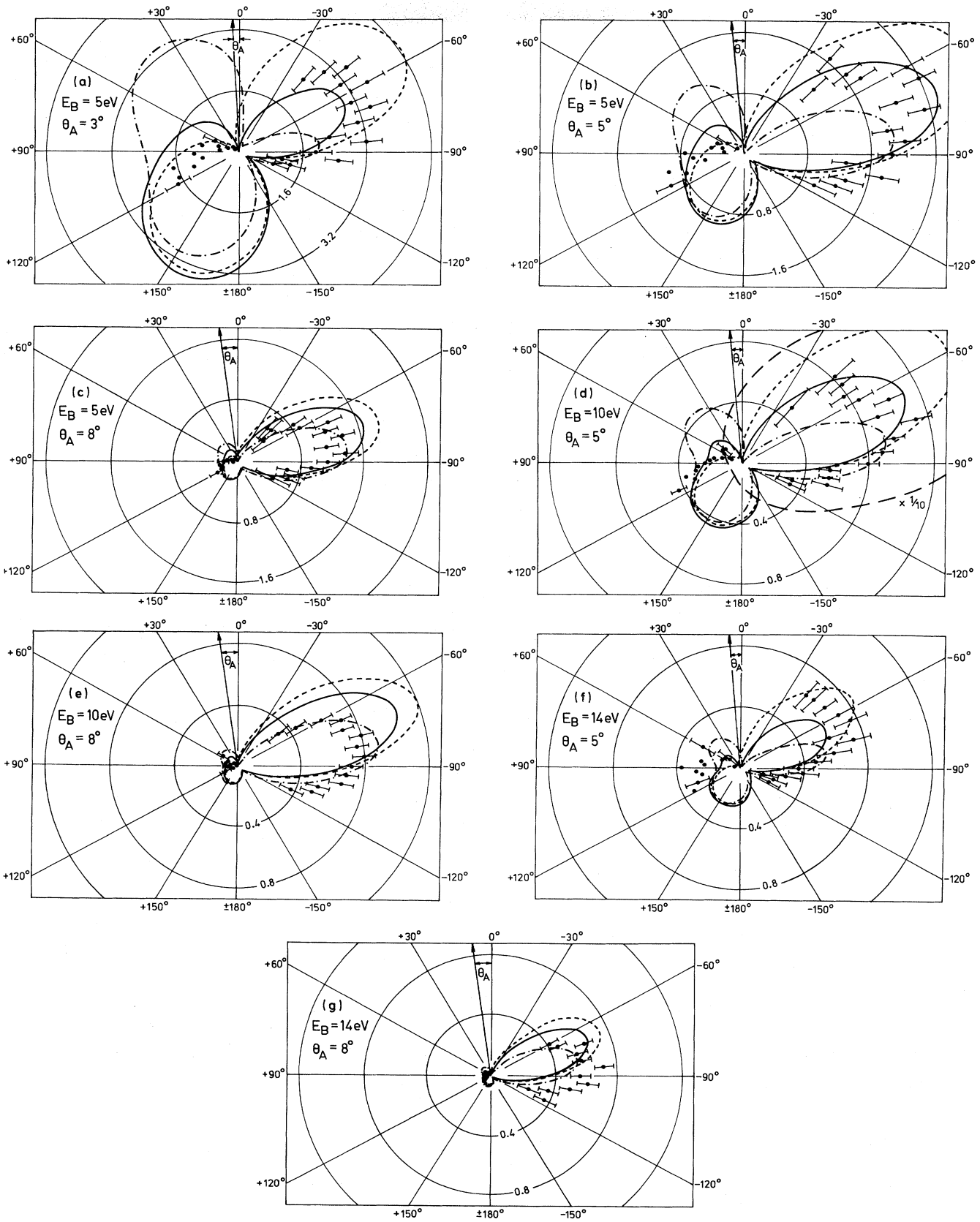

FIG. 3. Polar diagrams of the differential coplanar asymmetric $(e,2e)$ cross sections measured for atomic hydrogen at $E_0=250$ eV with $E_B=5$, 10, and 14 eV and $\theta_A=3°$, 5°, and 8°. Data have been normalized as discussed in the text. Calculated cross sections are ——, DWIA-I; — — —, DWIA-II; —·—·—·, DWIA-III; ———, PWIA.

TABLE II. Comparison of the momentum transfer direction θ_K and the angular position of the binary peak maximum as given by experiment and theory.

					Angular position θ_B of binary peak maximum					
E_B (eV)	θ_A (deg)	θ_K (deg)	K (a.u.)	Expt. (deg)	DWIA-I (deg)	DWIA-II (deg)	DWIA-III (deg)	$B1$ (deg)	$B2$ (deg)	EBS (deg)
5	3	52	0.27	63±5	63	53	84	52	63	63
5	5	64	0.40	69±2	70	63	83	64	71	71
5	8	71	0.61	78±2	73	71	82	71	77	77
10	5	58	0.42	70±2	65	58	80	58	66	66
10	8	67	0.62	81±2	70	69	78	67		
14	5	54	0.43	70±3	64	57	78	54		
14	8	63	0.63	84±2	68	64	79	63		

DWIA-I cross sections, and absence in the DWIA-II cross sections, shows that it is an effect produced by the distortion of the fast outgoing wave, since the incoming and slow outgoing electron waves are the same in all the calculations, and in the DWIA-II the fast outgoing electron is represented by a plane wave.

The plane-wave impulse approximation has been included in Fig. 3(d). As expected it produces no recoil peak. The magnitude of the cross section is also about 20 times greater than that given by the DWIA-I calculation.

Table II presents the magnitude and direction of the momentum transfer for each case and, for comparison, the angular position of the binary peak maximum as determined experimentally and as predicted by the various calculations. The "experimental" maxima were obtained by fitting the data with the calculated recoil peak shapes. Different cross-section shapes could yield different positions of the maximum in some cases. The more sophisticated calculations predict that the binary peak maximum should lie at larger angles θ_B than the momentum transfer direction $\theta(\vec{K})$, and are thus in better agreement with experiment. However, nearly all the calculations predict that the position of the binary peak should vary in the same way with varying slow-electron energy as does the momentum transfer direction, that is, the binary peak should move to smaller angles θ_B as E_B increases for a fixed value of θ_A. Experimentally we find that the binary peak appears to move to larger angles θ_B as E_B increases, an effect that is particularly noticeable at $\theta_A = 8°$.

SUMMARY

In conclusion one can say that the recent second-Born-approximation and eikonal-Born-series calculations of Byron, Joachain, and Piraux[13] give a very good fit to the data at the energies and angles at which the calculations are available. They do especially well for the case involving minimum momentum transfer (smallest scattering angle θ_A and energy E_B). However, except in this case, they predict recoil peaks which are significantly smaller than those observed experimentally. On the other hand, the distorted-wave impulse approximation is expected to be most accurate for situations involving very high momentum transfer. The DWIA-I calculation gives, however, a surprisingly good fit to the data, although the relative magnitudes are not always predicted accurately, and at $E_B = 10$ and 14 eV and $\theta_A = 8°$ the predicted binary peak is at a significantly smaller angle θ_B than observed experimentally.

The DWIA-II and DWIA-III calculations predict, respectively, a binary peak at smaller and larger angles θ_B than are predicted by the DWIA-I. In each case the DWIA-III predicts a double-lobe structure for the recoil peak which is not observed experimentally. The DWIA-I and -II calculations give a very good description of the recoil peak except for the minimum momentum transfer case.

In the absence of an exact solution of the Coulomb three-body problem the use of approximations to analyze electron-hydrogen ionization experiments gives important clues to the two-body quantities that are emphasized in various kinematic regions. It has been shown previously[4] that ionization events with outgoing energies not far from equal are excellently represented by the distorted-wave impulse approximation, where the two-electron quantity that is emphasized is the t matrix, which treats the two-electron collision to all orders. The electron-nucleus interaction emphasizes the interior of the interaction region where each electron is influenced by the full Coulomb potential of the nucleus. The kinematic situation is very different with the present experiments. The electrons do not approach each other as closely as in the more symmetric cases. Evidently the Born series, which emphasizes all potentials equally in each order, represents the binary peaks somewhat more accurately than the DWIA which strongly emphasizes the electron-electron collision. It is perhaps surprising that the DWIA works as well as it does. The effect of different distorting potentials for the fast outgoing electron gives more physical information about the process. The fast electron feels an effective central potential that is intermediate between zero (full screening) and the bare Coulomb potential of the nucleus (no screening). The ground-state average potential is a good, but not completely adequate, approximation to this.

ACKNOWLEDGMENTS

We thank with pleasure Professor C. J. Joachain for providing us, prior to publication, with the details of the Born-series calculations carried out by him, F. W. Byron, Jr., and B. Piraux. We are grateful to the Australian Research Grants Scheme for financial support of this work. B.L. acknowledges the support of a Commonwealth Postgraduate Research Award.

[1]B. Lohmann and E. Weigold, Phys. Lett. 86A, 139 (1981).
[2]I. E. McCarthy and E. Weigold, Phys. Rep. 27C, 275 (1976).
[3]E. Weigold and I. E. McCarthy, Adv. At. Mol. Phys. 14, 127 (1978).
[4]E. Weigold, C. J. Noble, S. T. Hood, and I. Fuss, J. Phys. B 12, 291 (1979).
[5]H. Ehrhardt, K. H. Hesselbacher, K. Jung, and K. Willmann, Case Stud. At. Phys. 2, 159 (1971).
[6]H. Ehrhardt, M. Fischer, K. Jung, F. W. Byron, Jr., C. J. Joachain, and B. Piraux, Phys. Rev. Lett. 48, 1807 (1982).
[7]H. Ehrhardt, M. Fischer, and K. Jung, Z. Phys. A 304, 119 (1982).
[8]E. C. Beaty, K. H. Hesselbacher, S. P. Hong, and J. H. Moore, J. Phys. B 10, 611 (1977).
[9]D. H. Madison, R. V. Calhoun, and W. N. Shelton, Phys. Rev. A 16, 552 (1977).
[10]K. L. Baluja and H. S. Taylor, J. Phys. B 9, 829 (1976).
[11]B. H. Bransden, J. J. Smith, and K. H. Winters, J. Phys. B 11, 3095 (1978).
[12]F. W. Byron, Jr., C. J. Joachain, and B. Piraux, J. Phys. B 15, L293 (1982).
[13]F. W. Byron, Jr., C. J. Joachain, and B. Piraux, Phys. Lett. 99A, 427 (1983).
[14]F. W. Byron, Jr. and C. J. Joachain, Phys. Rep. 34C, 233 (1977).
[15]I. E. McCarthy, C. J. Noble, B. A. Phillips, and A. D. Turnbull, Phys. Rev. A 15, 2173 (1977).
[16]J. P. Toennies, W. Welz, and G. Wolf, J. Chem. Phys. 71, 614 (1979).
[17]J. Slevin and W. Stirling, Rev. Sci. Instrum. 52, 1780 (1981).
[18]W. Mehlhorn and D. Stahlherm, Z. Phys. A 217, 294 (1968).
[19]T. W. Shyn and W. E. Sharp, Phys. Rev. A 19, 557 (1979).
[20]C. B. Opal, E. C. Beaty, and W. K. Peterson, At. Data 4, 209 (1972).
[21]Yong-Ki Kim, Phys. Rev. A 28, 656 (1983).